Food and Bioprocess Technology (2025) 18:6520–6536
https://doi.org/10.1007/s11947-025-03820-x

RESEARCH

# Improving the Long-Term Stability of Carotenoids from *Dunaliella Salina* Supercritical Fluid Extracts with a New Liposomal Encapsulation Based on Cryogenic and Stirring Processes

**Victor M. Amador-Luna[1] · Miguel Herrero[1] · Pablo Mendoza-Orbaneja[1] · Elena Ibáñez[1] · Lidia Montero[1]**

Received: 23 September 2024 / Accepted: 21 March 2025 / Published online: 21 April 2025
© The Author(s) 2025

**Abstract**
The search for new natural bioactive compounds has recently been intensified; however, some compounds are unstable under atmospheric conditions, suffering degradation and loss of bioactivity. Encapsulation is a strategy employed in the food industry to enhance the stability of such labile compounds. This study presents a novel microencapsulation method for preserving terpene-rich extracts from the microalga *Dunaliella salina* with potential neuroprotective activity. Microliposomes were formed using phosphatidylcholine as encapsulating agent, creating a nanoemulsion stabilized by lyophilization. A purification step yielded a pure encapsulated product with an efficiency of 63%. The behavior of key compounds, particularly terpenes and carotenoids, was analyzed throughout the encapsulation process. Low molecular weight terpenes were the most affected by processing temperatures, while carotenoid encapsulation was linked to their structure-concentration relationship. Stability tests under accelerated storage conditions (45 °C) revealed only a 20% reduction in bioactivity over three months, demonstrating high stability under extreme conditions.

**Keywords** Microliposomes · Encapsulation efficiency · Carotenoids · Stability · Neuroprotective activity

## Introduction

Terpenes, naturally occurring compounds with diverse structures, are found in plants and classified based on the number of isoprene units (C5 skeleton) into mono- (C10), sesqui- (C15), di- (C20), tri- (C30), or tetraterpenes (C40). They are responsible for the aromatic properties of plant essential oils and possess potential health benefits, including antioxidant, anti-inflammatory, and antimicrobial activities (Déclaire & Nzeuwa, 2021). Among them, tetraterpenoids (carotenoids) are crucial in the diet as they can act as vitamin precursors, such as β-carotene (Maoka, 2020). These compounds exhibit vibrant colors (yellow, orange, red, and purple) that enhance food organoleptic properties and are known for their antioxidant properties. Carotenoids have been linked to neuroprotective, hepatoprotective, anticancer, antidiabetic, and cardioprotective effects (Olatunde et al., 2020).

*Dunaliella salina*, a microalga, is renowned for its high carotenoid content, particularly β-carotene isomers. Carotenoids from *D. salina* have demonstrated antioxidant, anti-inflammatory, and anticholinergic properties, particularly when extracted using supercritical fluid extraction (SFE) and ultra-high pressure SFE (UHP-SFE) (Amador-Luna et al., 2024; Bueno et al., 2020). Our research group has focused on carotenoid-enriched extracts from *D. salina*, investigating their potential as neuroprotective functional ingredients (Amador-Luna et al., 2024; Bueno et al., 2020; Gallego et al., 2022; Valdés et al., 2024). These extracts, obtained under specific extraction conditions, show a highly enriched carotenoid profile, responsible for their biological activities.

However, terpenes, particularly carotenoids, exhibit sensitivity to light, oxygen, humidity, and temperature. This sensitivity can lead to rapid degradation post-extraction, reducing bioactivity (Mordi et al., 2020). Therefore, developing methods to preserve the bioactivity of these extracts is essential. Encapsulation is a promising technique to protect and maintain the functionality of bioactive compounds. Encapsulation can also improve the bioavailability and

✉ Lidia Montero
lidia.montero@csic.es

[1] Laboratory of Foodomics, Institute of Food Science Research, CIAL-CSIC, Nicolas Cabrera 9, 28049 Madrid, Spain

bioaccessibility of these compounds by providing protection during gastrointestinal digestion (Morris, 2014; Davidov-Pardo et al., 2013). Various encapsulation technologies are employed in the food industry, with physical microencapsulation techniques such as spray-drying, freeze-drying, extrusion, and supercritical fluid processes being among the most commonly used methods (Fang & Bhandari, 2010).

Recent methods include spray cooling, ionic gelation, solvent evaporation, liposome entrapment, and coacervation (Ozkan et al., 2019; Thies, 2012). Nanoencapsulation techniques, producing particle sizes between 10 and 1000 nm, are increasingly popular due to better gastrointestinal absorption of bioactives (Desai et al., 1996; Sobel et al., 2023). Lipid-based nanoparticles, such as nanoemulsions, liposomes, solid lipid nanoparticles, and nanostructured lipid carriers phytosomes, niosomes, glycerosomes or invasomes, are effective for terpene stabilization (Akanda et al., 2023; Andleeb et al., 2021; Cheng et al., 2022; Fei et al., 2023; Ge et al., 2019; Kaltschmidt et al., 2020; Lason, 2020; Zhang et al., 2017).

Liposome-based encapsulation is particularly effective for low-polarity compounds due to their amphiphilic nature, enhancing encapsulation efficiency and compound solubility. Liposomes, consisting of phospholipid bilayers, offer a safe, biocompatible option for food applications, protecting encapsulated compounds from degradation (Akram et al., 2023; Kosaraju et al., 2008). The USFDA supports liposome use, highlighting their protective abilities against pH, light, digestive enzymes, and cellular interactions (FDA, 2018).

This study aims to develop a novel encapsulation process to protect and enhance the stability of a terpene-rich extract from *D. salina* using UHP-SFE, assessing encapsulation efficiency and comparing neuroprotective activity with the crude extract. Moreover, a detailed evaluation of the effect of each encapsulation step over the composition of the bioactive extract has been provided, being the first time that this kind of encapsulation is carried out in a complex high-hydrophobic extract.

## Materials and Methods

### Samples and Reagents

The microalga *Dunaliella salina* was obtained from Algalimento (Las Palmas de Gran Canaria, Spain). The biomass was provided as a lyophilized powder (particle size < 100 µm).

All the solvents and reagents used for the extraction, bioactivities measurements, and LC and GC analysis are described in Amador-Luna et al. (2024). Soy phosphatidylcholine from lecithin for the liposomal formation was provided by Thermo Scientific GmbH (Karlsruhe, Germany).

### Supercritical Fluid Extraction

Terpene extraction from *D. salina* was conducted using a semi-pilot scale SFE system (SFE lab 2L, SFE-Process, Tomblaine, France) with an optimized UHP-SFE method (Amador-Luna et al., 2024). The extraction cell contained 350 g of biomass and 700 g of glass beads. Purified $CO_2$ was pumped at a flow rate of 60 g $min^{-1}$ for 1 h, under conditions of 84.9 MPa pressure and 45 °C temperature. This extract served as the starting material for encapsulation. Figure 1A displays a microscopic image of the initial UHP-SFE extract.

### Liposomal Microencapsulation Preparation and Microliposome Purification

The developed encapsulation methodology consisted of several steps, as can be seen in Table 1: (I) phosphatidylcholine (1 g) was mixed with 49 g of hot deionized water (80 °C) and stirred at 300 rpm for 1 h using a Thermomixer (Thermomixer comfort 50 mL, Eppendorf Iberica, Madrid, Spain) to create the liposomal suspension (in triplicate); (II) the terpene-rich extract was dissolved in ethanol, then it was added after the first stirring step to obtain a final concentration of 2000 ppm of extract. The mixture was stirred at the same speed for 2 h at 60 °C to create a nanoemulsion (Oskoueian et al., 2020). Figure 1B shows the microscopic images of the resulting nanoemulsion; (III) the nanoemulsion was sonicated in an ultrasonic system Elmasonic S10 (Elma, 01006, Vitoria, Alava, Spain) for 15 min to obtain the nanoliposomes; (IV) a new step was added at this point consisted of the lyophilization of the microliposomes. The microliposomes were frozen at – 80 °C, and lyophilized in a freeze-dryer (Alpha LSCbasic, CHRYST, Osterode am Harz, Germany) for 72 h to obtain the stabilized microliposome mixture (Fig. 1C). To observe the contrast between stabilized microliposomes with and without extract, the same described process was performed but without adding the starting UHP-SFE extract (Fig. 1D). After drying, the product was stored at – 20 °C until used.

After the four previous steps, a purification of the stabilized microliposome mixture was carried out to eliminate, on one hand, the free phosphatidylcholine that remained after encapsulation, and, on the other hand, to remove the non-encapsulated extract. To do that, the following steps were followed: (V) the stabilized microliposome mixture was reconstituted with deionized water (1:10 *w/v*) by suspending the mixture for 1 h under continuous stirring at 5 G. After this period, the reconstituted microliposomes were centrifuged at 50,000 G in an ultracentrifuge (Fiberlite, Thermo Fisher Scientific, Grand Island, NY, USA) for 10 min at 4 °C (Beyrami et al., 2020). The generated supernatant (free phosphatidylcholine) was eliminated. The pellet after the phosphatidylcholine elimination consisted of a mixture of encapsulated

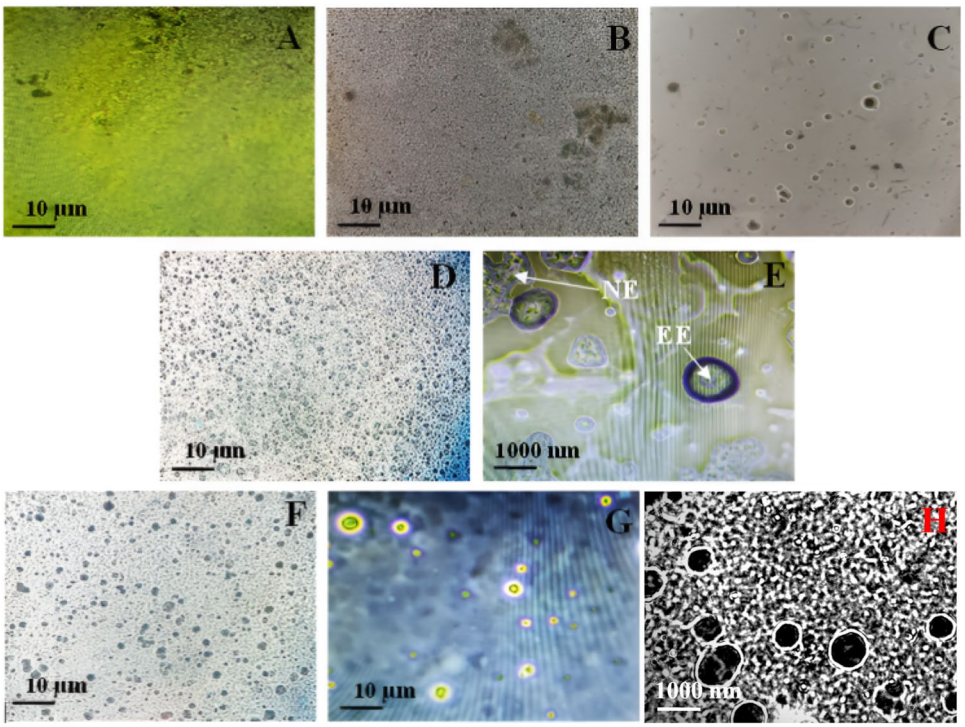


**Fig. 1** Microscopic images of the resulting products corresponding to different encapsulation steps: **A** Phase-Contrast image of starting UHP-SFE extract. **B** Microemulsion (steps I + II), **C** stabilized microliposome mixture (step IV), **D** stabilized microliposomes without UHP-SFE extract. **E** Phase-Contrast image of the non-purified encapsulated mixture showing liposomes with extract (EE) with monolayer structure, and non-encapsulated extract (NE) (step V). Encapsulated product (step VI) under microscopic (**F**), phase-contrast image (**G**) and non-polarized light with black and white contrast (**H**)

product and non-encapsulated extract (non-purified encapsulated mixture) (Fig. 1E); (VI) the pellet corresponding to the non-purified encapsulated mixture was resuspended in ethanol (1:10, *w/v*) under continuous stirring at 300 rpm for 1 h to dissolve the free non-encapsulated extract. The mixture was again centrifuged at 50,000 G and the supernatant (non-encapsulated fraction) was separated and stored at – 20 °C for encapsulation efficiency analysis. This step resulted in the encapsulated product that was dried using a speed-vac SPD-1030 Integrated Vacuum Concentrator (Thermo Fisher Scientific, Grand Island, NY, USA) for 2 h and stored at - 20 °C until used (Fig. 1 F, G, and H). The microphotographs taken at different encapsulation steps (Fig. 1) were made using a Leica optical microscope Dmi1 coupled to a digital camera Flexacam C1 (Leica Microsystems CMS GmbH, Ernst-Leitz-Str, 17–37, D-35578 Wetzlar).

## Encapsulation Efficiency of the Extract

To calculate the total encapsulation efficiency, the ethanolic supernatant (containing the non-encapsulated fraction) was dried using a speed-vac for 2 h and the resulting dried sample was weighed. The encapsulation efficiency (EE) was calculated using Eq. 1.

$$EE(\%) = \frac{\text{Startingextract(mg)} - \text{non} - \text{encapsulatedfraction(mg)}}{\text{Startingextract(mg)}} \cdot 100\% \quad (1)$$

Then, the encapsulation efficiency of each compound and family of compounds was calculated, i.e., the encapsulation efficiency was represented in terms of total terpene content (TTC), individual terpenes, total carotenoid content (TCC), and individual carotenoids following the protocols detailed in Amador-Luna et al. (2024). The encapsulation efficiency of TCC and TTC is described in Supplementary Material S2 and S3.

## Total Terpene Content

For the TTC calculation, the extract was prepared at 250 mg $mL^{-1}$ in EtOH. Then 200 µL of this solution were mixed with 1.5 mL of $ChCl_3$ and vortexed (30 s). The samples were placed in an ice-bath and 100 µL of sulfuric acid were added to each sample. The mixture was gently tilted, then incubated in darkness for 2 h. Following the same procedure, a calibration curve of limonene was prepared (31–500 mg $mL^{-1}$ in EtOH) reducing the incubation time to 5 min. After the incubation, the supernatant was removed and the resulting reddish precipitate was diluted in 1.5 mL of EtOH and analyzed in an absorbance spectrophotometer at 528 nm (Synergy HT, BioTek Instruments, Winooski, VT, USA).

### Total Carotenoid Content

The extract was dissolved in cold acetone/water (90:10, *v/v*) at 0.05 mg $mL^{-1}$ and stored in the dark at 4 °C overnight. Then, the mixture was centrifuged at 1500 G (4 °C, 10 min). After that, the supernatant was recovered and diluted with 5 mL acetone acetone/water (90:10, *v/v*) and the absorbance was measured at 480 and 750 nm. The value of TCC was obtained following the calculations described in Amador-Luna et al. (2024).

### Characterization of the Individual Terpenes

The individual terpenes were tentatively identified by a GC–MS (Shimadzu Corporation, Kyoto, Japan). The column to perform the separation was Zebrom ZB-5Plus (30 m × 250 µm i.D × 0.25 µm, Phenomenex, Torrance, CA, USA) using helium as carrier gas (0.8 mL $min^{-1}$). More details about the GC separation can be found in section S4.

### Characterization of the Individual Carotenoids

The chemical carotenoid composition was performed in an Agilent 1100 series liquid chromatograph (Santa Clara, CA, USA). The selected column for the separation was a YMC-C30 reversed phase column (250 mm × 4.6 mm i.d., 5 µm particle size; YMC Europe, Schermbeck, Germany) and a pre-column YMC-C30 (10 mm × 4 mm i.d., 5 µm particle size). The separation was performed using methanol/MTBE/water (90:7:3 *v/v/v*) as mobile phase A and methanol/MTBE (10:90 *v/v*) as mobile phase B at a flow rate of 0.8 mL $min^{-1}$. The complete LC-DAD-MS/MS method is described in section S5.

### Bioactivity Assays and In Vitro Characterization

To assess their bioactivity, all samples were diluted in ethanol (EtOH). The encapsulated product was homogenized in EtOH using a Potter–Elvehjem glass homogenizer with a PTFE pestle to release the extract by breaking the encapsulation until the pellet mass lost its color. The mixture was then centrifuged at 5500 G for 5 min at 4 °C using a Mikro 120 centrifuge (Hettich, Tuttlingen, Germany). Detailed procedures are provided in Section S1 of the Supplementary Material. The supernatant was extracted with EtOH and used for bioactivity assays, including antioxidant, anti-inflammatory, and anti-cholinergic activities following the protocols described in Amador-Luna et al. (2024). The protocols for these bioassays are described in section S6. All assays were conducted in a 96-well microplate using a Cytation 5 imaging reader with an auto-disperser (BioTek Instruments, Winooski, VT, USA).

### Evaluation of the Microencapsulation Process Effects on *D. salina* Compounds by GC–MS and HPLC–DAD-MS/MS

To assess the potential impact of each step of the microencapsulation process on the bioactivity and composition of the terpene-rich extract, aliquots of the supernatant were collected after homogenization at each stage of the process. These samples were analyzed using GC–MS/MS and HPLC–DAD-MS. The methods used for both chromatographic techniques are described in Amador-Luna et al. (2024). The GC–MS and the HPLC–DAD-MS methods are detailed in sections S5 and S6, respectively. The specific fractions examined included (i) the stabilized microliposome mixture, (ii) the non-purified encapsulated mixture, and (iii) the final encapsulated product. All fractions were analyzed under the same conditions as the starting extract to monitor changes in the content and composition throughout the process.

For the GC–MS analysis of terpenes and other volatile compounds, the samples were analyzed in triplicates, determining the encapsulation efficiency of each identified compound using the following formula (Eq. 2).

$$EE_{VolComp}(\%) = 1 - \frac{A_i - A_f}{A_i} \cdot 100\% \quad (2)$$

where $EE_{VolComp}$ is the encapsulation efficiency of each individual compound present, Ai is the area in the starting UHP-SFE extract and Af is the compound area in the encapsulated fraction.

The LC method was used for the analysis of carotenoids of both, the starting extract and the encapsulated product (10 times higher concentrated in comparison to the starting extract) in triplicate, determining the encapsulation efficiency of each carotenoid using the following formula (Eq. 3).

$$EE_{i,carot}(\%) = 1 - \frac{A_i - A_f}{A_i} \cdot 100\% \quad (3)$$

where EEi, carot is the encapsulation efficiency of each individual carotenoid, Ai is the carotenoid area in the starting UHP-SFE extract, and Af is the carotenoid area in the encapsulated fraction.

### Stability Study

The stability of both the starting SFE extract (without encapsulation) and its encapsulated product was evaluated under two different conditions. Firstly, both the SFE extract and

the encapsulated product were subjected to a simple stability study under atmospheric conditions (21 °C, 0.1 MPa, and 50% relative humidity) over the course of 1 month, with measurements taken weekly. Additionally, the encapsulated product was stored under accelerated conditions (45 °C and 0.1 MPa) for 3 months, with measurements taken monthly. To assess stability, total carotenoid content (TCC), and anticholinergic activity (AChE inhibition) were measured, using the methods detailed in Supplementary Material sections S3 and S4.3.

### Statistical Analysis

All the analyses were performed in triplicate. SPSS vs. 19 (IBM) was used for the statistical analysis of the results. One-way ANOVA analysis ($p$ values $< 0.05$) was applied to evaluate the significant differences and then, Fisher's exact test was carried out.

## Results and Discussion

This study presents, for the first time, the development of a microencapsulation process using phosphatidylcholine-based liposomes specifically designed for the encapsulation of hydrophobic natural extracts. Figure 2 shows an outline of the complete process carried out for the encapsulation procedure and the evaluations performed in each step of this process.

### Microencapsulation for Terpene-Rich UHP-SFE Extracts from *D. salina* Biomass

In this study, a terpene-rich extract from the microalga *Dunaliella salina* was obtained using UHP-SFE. This extract, particularly rich in β-carotene and other carotenoids (Amador-Luna et al., 2024; Bueno et al., 2020), required an encapsulation method that could effectively retain, protect, and release the bioactive compounds. Phosphatidylcholine was selected as the encapsulating agent owing to its capacity to form liposomes and its potential neuroprotective benefits, such as enhancing neuronal plasticity and reducing neuroinflammation (Magaquian et al., 2021). Other substances were deemed unsuitable for being non-food-grade or having poor nutritional value, including hydrogenated fats and various lipid types.

A microencapsulation technique was selected to produce particles smaller than 100 µm, which are more easily absorbed in the gastrointestinal tract (Desai et al., 1996). This process aimed to create micro- and nano-structures (10 µm to 10 nm) suitable for encapsulating terpenoids by forming emulsions (Oskoueian et al., 2020). Hydrophobic components were incorporated into nanocapsules by aligning their hydrophobic tails inward and polar heads toward the aqueous medium. The resulting structures included inclusion complexes and single or multilayer oil-in-water (O/W) emulsions.

The encapsulation process, as detailed in "Liposomal microencapsulation preparation and microliposome purification" section, involved three critical steps (Table 1., Fig. 1):

Freeze-drying (Step IV): This step was added to remove moisture from the micro- and nano-structures containing the extract. After achieving a stable O/W nanoemulsion of the extract in an aqueous medium with phosphatidylcholine, moisture was removed via lyophilization. In this work, this step was included instead of the use of hot-air that is normally used in this kind of encapsulation method. The main reason for this substitution was that hot-air drying could degrade carotenoids due to the use of high temperatures considering that carotenoids may degrade at temperatures higher than 40 °C. Therefore, freeze-drying reduced the possible thermal degradation of the terpenes present in the sample. Lyophilization resulted in a stabilized microliposome mixture containing free phosphatidylcholine, encapsulated extract, and non-encapsulated fractions.

Rehydration of stabilized microliposome mixture (Step V): To eliminate excess encapsulating agent, the freeze-dried liposomes were rehydrated with gentle stirring at 5 G, preventing temperature increases. Ultra-centrifugation at 50,000 G (Oskoueian et al., 2020) then separated the phosphatidylcholine excess from the encapsulated extract. The supernatant was discarded, resulting in a pellet of encapsulated extract and non-encapsulated extract, forming a non-purified encapsulated mixture (Table 1., Fig. 1E).

Purification of non-purified encapsulated mixture (Step VI): To remove the non-encapsulated fraction, the mixture was treated with ethanol, which solubilized the non-encapsulated extract. The supernatant containing this fraction was separated via centrifugation. Vacuum drying was preferred for solvent evaporation, as it was faster and did not damage the liposome membrane, unlike nitrogen stream evaporation, which caused membrane rupture. This method yielded a final dried encapsulated product suitable for storage under atmospheric conditions.

Following encapsulation, various parameters were examined to determine the feasibility and success of the process. These included encapsulation efficiency, bioactivity of the encapsulated extract, the impact of encapsulation on the extract's chemical composition, and the stability of the encapsulated product.

#### Encapsulation Efficiency

The total encapsulation efficiency of the process was calculated as a percentage of the total starting extract weight and after the reconstitution of the encapsulated product in ethanol. The total encapsulation efficiency of the *D. salina* UHP-SFE

**Table 1.** Microliposome encapsulation process of the *D. salina* UHP-SFE extract

| | Step | Process | Result | |
|---|---|---|---|---|
| Microliposome preparation | I+II | Mixture of phosphatidylcholine, water and starting terpene-rich extract 2000 ppm – 60ºC – 2 h | **Microemulsion** (Figure 1B) | 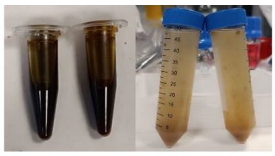 |
| | III | Ultrasonication 40 Hz – 15 min | **Microliposomes** | |
| | IV | Lyophilization 72 h | **Stabilized microliposome mixture** (Figure 1C) | 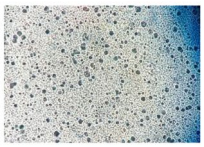 |
| Microliposome purification | V | Elimination of free phosphatidylcholine Water - 1 h – 5 G Centrifugation 50000 G – 10 m | **Non-purified encapsulated mixture** (mix of encapsulated and non-encapsulated extract) (Figure 1E) | 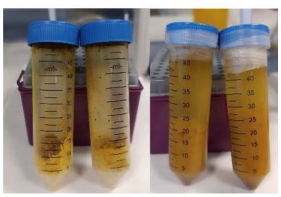 |
| | VI | Separation of the non-encapsulated extract Ethanol - 1 h – 5 G Centrifugation 50000 G – 10 min | • **Non-encapsulated fraction** • **Encapsulated product** (Figure 1F, 1G, 1H) | |

extract was 63 ± 5%. The encapsulation efficiency achieved in this process was in the range of the usual values achieved for this kind of encapsulation technique (usually between 40 and 80% efficiency). However, the encapsulation methodology developed in this work presented a lower variability showing to be a more robust process.

The most critical factors that may affect the efficiency of the encapsulation process were temperature, pores formation, and time. Specifically, the initial stage of the nanoemulsion formation (60 °C) can affect the stability of volatile and thermolabile compounds due to the absence of nanocarriers that allow the fixation of bioactive compounds during the emulsion formation process (Rostamabadi et al., 2019). On the other hand, freeze-drying processes can also reduce the encapsulation efficiency due to the destabilization and disruption of the formed micro- or nanostructures, and the increase in the size of the pores present in the nanostructures which, in turn, might favor the initiation of the degradation of the exposed molecules (Lavelli & Sereikaitè, 2022). To our knowledge, this is the first work showing the application of this kind of encapsulation process for complex natural extracts, instead of pure molecules. Having in mind the complexity involved in this kind of extract in terms of chemical composition and properties, besides the satisfactory encapsulation efficiency achieved, it is necessary to evaluate the effect that the different steps produce on the native compounds to ensure the quality of the encapsulated extract.

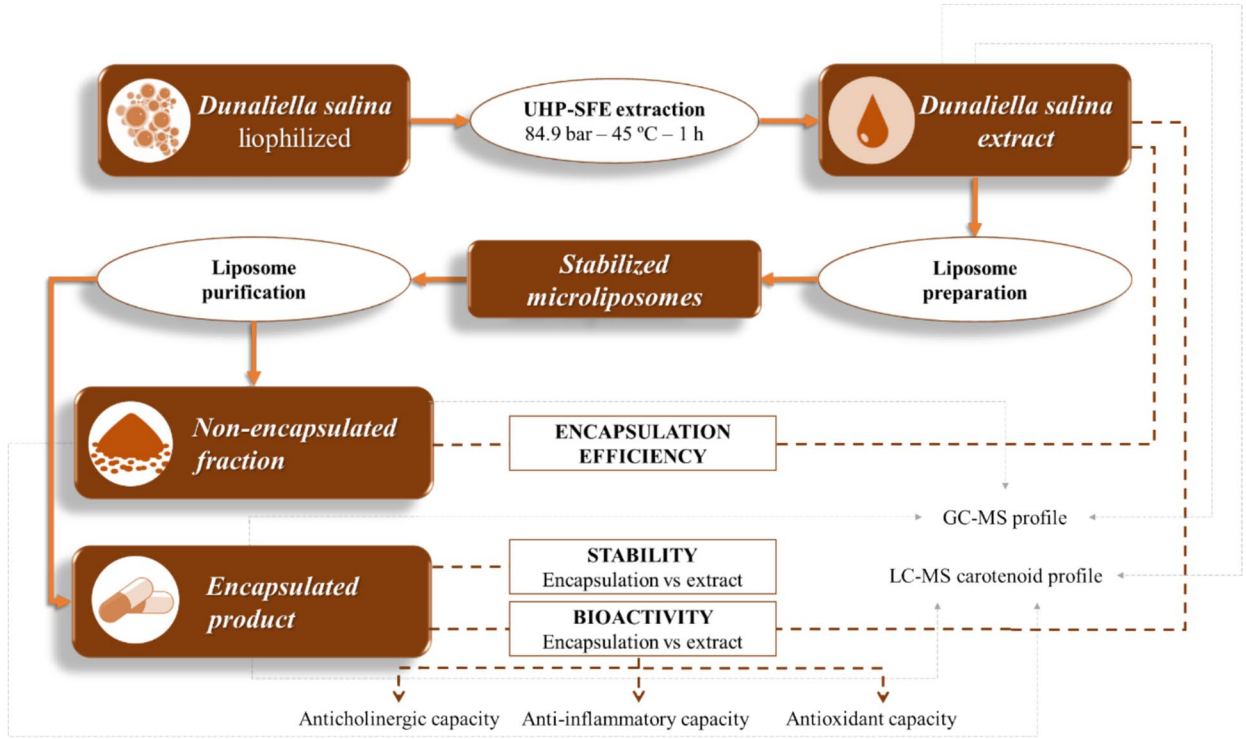


**Fig. 2** Procedure employed to carry out the microencapsulation process and the study of the encapsulated extract (encapsulation efficiency, bioactivity, composition and stability)

### Effect of the Encapsulation Process on the Carotenoid Profile

To gain more insight into the behavior of the most relevant components present in the extract, the encapsulation efficiency was also estimated for total terpenes and total carotenoids (Fig. 3). The encapsulated extract showed a total terpene content of $1035.08 \pm 6.42$ mg-eq limonene $g^{-1}$ extract (Fig. 3A), and a total carotenoid content of $39.18 \pm 3.69$ mg-eq β-carotene 100 $mg^{-1}$ extract (Fig. 3B). Comparing these values with those determined in the starting UHP-SFE extract ($1628.20 \pm 21.98$ mg-eq limonene $g^{-1}$ extract for TTC, and $69.92 \pm 0.52$ mg-eq β-carotene 100 $mg^{-1}$ extract, for TCC), the encapsulation efficiency was 64% and 56% for total terpenes and total carotenoids, respectively. These values were in line with the overall encapsulation efficiency previously determined. The loss of efficiency observed in the case of carotenoids might be due to a β-carotene partial degradation caused by the use of high temperatures (60 °C) in the initial stage of the nanoemulsion formation.

To better understand the encapsulation process of terpenes and carotenoids, the encapsulation behavior of the individual compounds of each group was evaluated and their encapsulation efficiency was also calculated. Regarding carotenoids, the compounds contained in the encapsulated product, previously dissolved in ethanol, were analyzed by LC–MS and compared to the starting UHP-SFE extract, as well as to the non-encapsulated fraction. Figure S1 illustrates the carotenoid profiles obtained for each fraction analyzed (starting extract (Fig. S1 A), non-encapsulated fraction (Fig. S1 B), and encapsulated product (Fig. S1 C)). After the quantitative analysis of the obtained chromatograms (Table 2), a total encapsulation efficiency for the separated photosynthetic pigments of 51% was observed. This value was close to the value calculated with TCC assay (56%). This result demonstrates that, in this case, the use of colorimetric assays for calculating the encapsulation efficiency could be highly representative of the overall encapsulation efficiency of the major components presented in the extract, being a simpler, cheaper and faster measurement. As can be observed from the chromatograms shown in Fig. S1 B and C and Table 2, all carotenoids were affected in a similar way after encapsulation, presenting encapsulation efficiencies of around 50%. Zeaxanthin, cryptoxanthin and *9-cis*-β-carotene (Peaks 2, 4, and 11, respectively), were the exceptions, presenting higher encapsulation efficiencies (72, 86, and 86%, respectively). The method used for the analysis of carotenoids also allowed the analysis of other natural pigments such as chlorophylls. Interestingly, the chlorophyll was detected in the starting extract (peak 5) was not observed in the non-encapsulated fraction (Fig. S1 B), which could

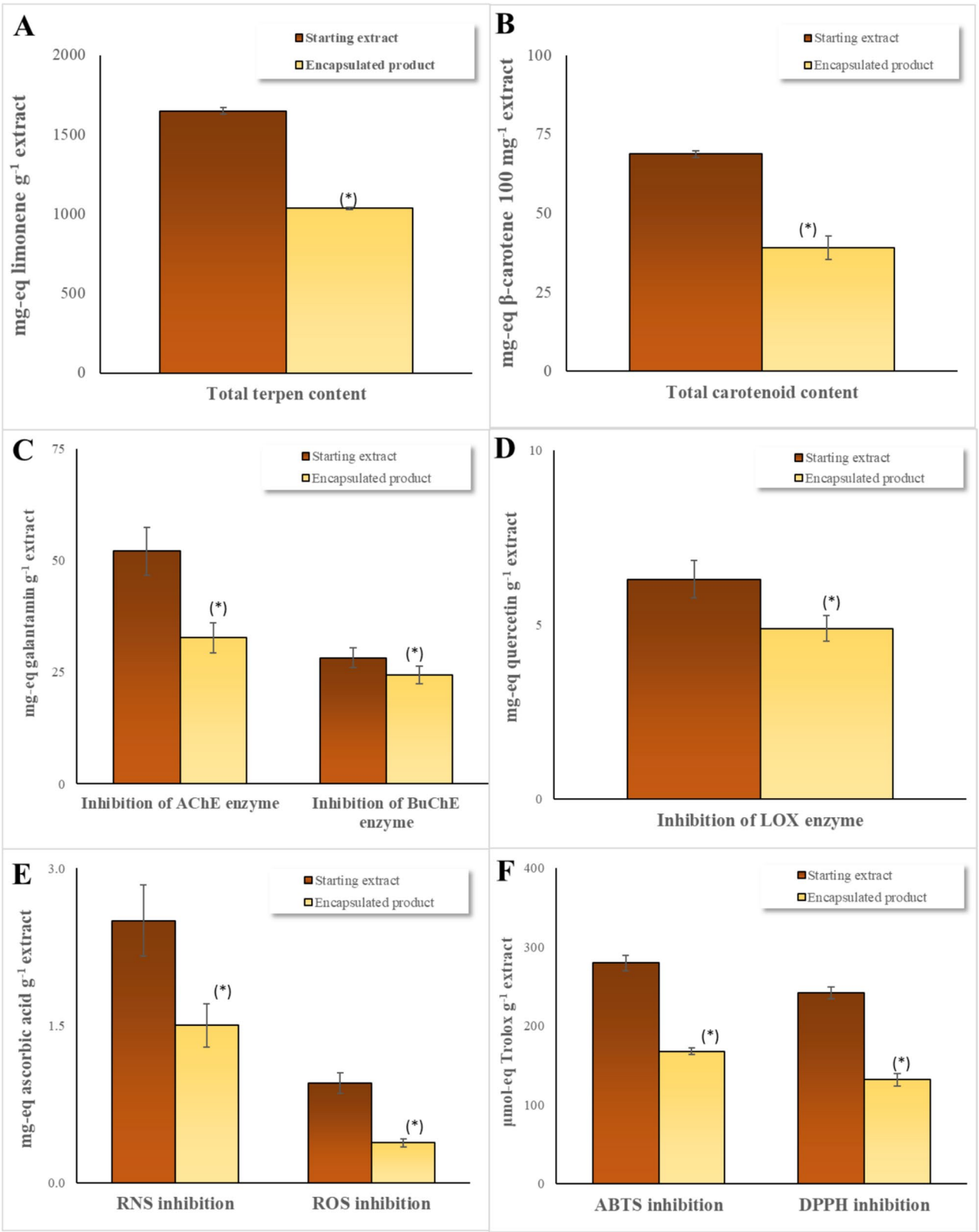
A
Starting extract
Encapsulated product
mg-eq limonene g-1 extract
2000
1500
1000
500
0
(*)
Total terpen content
B
Starting extract
Encapsulated product
mg-eq β-carotene 100 mg-1 extract
100
75
50
25
0
(*)
Total carotenoid content
C
Starting extract
Encapsulated product
mg-eq galantamin g-1 extract
75
50
25
0
(*)
(*)
Inhibition of AChE enzyme
Inhibition of BuChE enzyme
D
Starting extract
Encapsulated product
mg-eq quercetin g-1 extract
10
5
0
(*)
Inhibition of LOX enzyme
E
Starting extract
Encapsulated product
mg-eq ascorbic acid g-1 extract
3.0
1.5
0.0
(*)
(*)
RNS inhibition
ROS inhibition
F
Starting extract
Encapsulated product
µmol-eq Trolox g-1 extract
400
300
200
100
0
(*)
(*)
ABTS inhibition
DPPH inhibition

◂**Fig. 3** UHP-SFE extract and encapsulated extract content of **A** total terpenoids (mg-eq limonene $g^{-1}$ extract) and **B** total carotenoids (mg-eq β-carotene 100 $mg^{-1}$ extract) for the starting *D. salina* extract (brown) and the encapsulated product (yellow). In vitro neuroprotective assessment: **C** anticholinergic capacity against AChE and BuChE enzymes; **D** anti-inflammatory capacity against LOX enzyme; **E** antioxidant RNS and ROS scavenging, and **F** Trolox equivalent antioxidant capacity against ABTS and DPPH radicals. (*) indicates significant differences ($p$ value < 0.05) between the starting extract and the encapsulated product

confirm that the encapsulation of this compound was nearly 100%. This high efficiency of the chlorophyll and some xanthophylls could be due to their higher affinity to water compared to carotenes, which allowed greater stability during the heating applied to obtain the nanoemulsion.

The encapsulation efficiency for most of the β-carotene isomers was correlated with the concentration of each isomer in the sample, showing a better efficiency for those isomers with a higher concentration. However, this trend was not followed in the case of 15-*cis*-β-carotene (peak 10), which exhibited the lowest encapsulation efficiency (32%) albeit being the major compound within the sample. This behavior showed that the efficiency is not only correlated to the concentration of the carotenoid compounds but also with their isomer inherent structure.

Therefore, the encapsulation efficiency for carotenoids could be associated to their structure-concentration relationship more than each of them separately. This opens the door to new studies in order to fully understand the selectivity observed for the different carotene isomers and to predict the encapsulation efficiency of the compounds in order to know the behavior in complex matrices such as the one used in this work.

Table 2 also shows the comparison of the peak areas for each individual pigment identified in the starting UHP-SFE extract and in the non-encapsulated fraction and encapsulated product. No significant differences were observed for most of the compounds between the values before (starting extract) and after the encapsulation process (sum of each compound in the non-encapsulated fraction and the encapsulated product). These results indicate that, during the entire encapsulation process, the involved factors, including the temperatures and time used during the emulsion and freeze-drying steps did not affect the overall chemical composition of the extract and there was no loss/destabilization or oxidation of bioactive compounds, preserving the same profile before and after the entire process.

### Effect of the Encapsulation Process on the Terpene Profile

As mentioned in the previous section, the most critical points throughout the encapsulation process are those related to process temperature. Particularly, for the nanoemulsion formation step, the temperature is maintained at 60 °C for a period of 2 h, which could affect the most labile and volatile compounds, favoring their thermal degradation. To evaluate how the temperature in this step affected the composition of the compounds present in the extract, the non-encapsulated fraction, the encapsulated product as well as the starting UHP-SFE extract were analyzed by GC–MS. The results obtained in these GC–MS analysis correspond then to the relative quantification of small volatile terpenes, without considering the quantification of bigger terpenes such as carotenoids. The obtained chromatograms are shown in Fig. S2. Peak assignments and their relative amounts are summarized in Table 3.

Significant differences could be observed between the starting extract (Fig. S2 A) and the encapsulated product (Fig. S2 C) with all the determined peaks showing very low encapsulation efficiency values. To understand if the loss of compounds in the encapsulated product was due to a degradation process or to a low encapsulation affinity, the non-encapsulated fraction was also analyzed. Comparing the profile of the encapsulated product (Fig. S2 C) and non-encapsulated fraction (Fig. S2 B), it can be observed that many compounds could not be encapsulated since the profile of the non-encapsulated fraction was more complex, especially for the most volatile compounds. The low encapsulation efficiency of terpenes could be related to the nature of these components, having short chains and low molecular weights, which could favor their diffusion through the pores of the micelles or through the phospholipid layer itself (Harnkarnsujarit et al., 2012). It is worth highlighting the increase in encapsulation efficiency as the molecular weight of the terpenes increased (especially in triterpene compounds). This fact may corroborate that low molecular weight compounds are less retained inside the liposomes. But on the other hand, comparing the profile of the non-encapsulated fraction (Fig. S2 B) with the starting extract (Fig. S2 A), substantial losses of most of the components occurred during the encapsulation process, since both, the complexity and the abundance of these compounds was reduced during the encapsulation. These results could correspond most probably to a degradation suffered during the thermal processes carried out during the encapsulation. A practically total loss of the volatile compounds was observed after the encapsulation process (Table 3).

To further investigate which step in the encapsulation process could be responsible for the observed losses, the original extract and fractions generated after each encapsulation step were characterized. Figure S3 shows the chromatograms of the starting UHP-SFE extract compared to the fractions obtained after the three critical steps—i.e., (i) emulsion and lyophilization (steps II–IV), (ii) reconstitution (step V), and (iii) purification of the encapsulation (step VI). Besides, the results in terms of areas for each

**Table 2** LC–MS identification and total peak area of carotenoids found in the starting UHP-SFE extract, the non-encapsulated fraction and the encapsulated product obtained from *D. salina*, including also the encapsulation efficiency (in brackets) after the cryo-stirred microencapsulation process

| Peak ID | Rt (min) | Identification | $[M+H]^+$ (*m/z*) | Fragments (*m/z*) | λ max absorption (nm) | Peak area | | | |
|---|---|---|---|---|---|---|---|---|---|
| | | | | | | Starting UHP-SFE extract | Non-encapsulated fraction | Encapsulated product (Encapsulation efficiency) | Sum of the non-encapsulated and encapsulated fractions |
| 1 | 7.58 ± 0.15 | *Lutein* | 569.5 | 551.5, 533.1, 459.1 | 503, 465, 440 | 862.52 ± 33.94 | 362.52 ± 3.39 | 451.48 ± 54.96 (52%) | 814 ± 58.35 |
| 2 | 9.29 ± 0.05 | *Zeaxanthin* | 569.0 | 551.0, 477.1, 459.1, 416.0, 135.0 | 514, 476, 453 | 1120.00 ± 24.87 | 310.00 ± 2.49 | 809.01 ± 13.40 (72%) | 1119.01 ± 15.89 |
| 3 | 11.78 ± 0.22 | *n.i* | 565.3 | nd | 485, 475, 470 | 1494.95 ± 188.48 | 794.95 ± 18.85 | 477.17 ± 15.41 (32%) | 1272.12 ± 34.26* |
| 4 | 15.44 ± 0.26 | *Cryptoxanthin* | 553.0 | 535.1 | 478, 451 | 1551.13 ± 124.41 | 155.11 ± 12.44 | 1334.67 ± 31.68 (86%) | 1489.78 ± 44.12 |
| *5* | 17.70 ± 0.35 | *Chlorophyll-a* | 893.1 | 638.9, 589.7, 459.3 | 662, 430, 410 | 551.59 ± 56.20 | n.i | 543.25 ± 8.07 (98%) | 543.25 ± 8.07 |
| 6 | 26.07 ± 0.12 | *13-cis-β-carotene* | 537.5 | 444.4, 326.3. 272.2, 137.1, 121.1 | 465, 439 | 466.24 ± 19.30 | 266.24 ± 19.30 | 213.91 ± 4.39 (46%) | 480.15 ± 23.69 |
| *7* | 28.15 ± 0.03 | *all-trans-α-carotene* | 537.0 | 481.1, 444.1 | 478, 445,425 | 751.87 ± 8.86 | 351.87 ± 8.86 | 356.20 ± 25.53 (47%) | 708.07 ± 34.39* |
| 8 | 29.30 ± 0.14 | *9-cis-α-carotene* | 537.0 | 444.0 | 479,446,422 | 631.55 ± 7.16 | 331.55 ± 7.16 | 307.77 ± 3.43 (49%) | 639.32 ± 10.59 |
| 9 | 30.77 ± 0.26 | *all-trans-β-carotene* | 537.4 | 457.4, 400.3, 269.1, 137.1 | 472, 446 | 2667.70 ± 21.82 | 1067.70 ± 21.82 | 1438.53 ± 54.68 (54%) | 2506.23 ± 76.50* |
| *10* | 33.04 ± 0.11 | *15-cis-β-carotene* | 537.3 | 457.3, 137.0 | 466, 443 | 14,579.22 ± 200.92 | 9579.22 ± 200.92 | 4645.61 ± 58.14 (32%) | 14,224.83 ± 259.06 |
| *11* | 34.44 ± 0.12 | *9-cis-β-carotene* | 537.0 | 326.0, 137.1, 121.1 | 475, 450 | 5688.54 ± 195.41 | 688.54 ± 19.54 | 4871.38 ± 43.99 (86%) | 5559.92 ± 63.53 |
| | | | | | $\Sigma_{\text{total area}} =$ | 29,502.77 ± 847.43 | 13,545.16 ± 311.38 | 14,997.50 ± 781.02 (51%) | 28,542.66 ± 1092.40 |
| | | | | | $\Sigma_{\text{total area β-carotene isomers}} =$ | 24,785.15 ± 258.04 | 12,285.12 ± 277.60 | 11,833.4 ± 190.03 (47%) | 24,118.52 ± 467.63 |

Significantly different between the areas of the original UHP-SFE extract and the sum of the carontenoids present in the non-encapsualted fraction and the encapsulationon product

**Table 3** GC–MS identification, total peak area, and retention time of volatile compounds found in the starting UHP-SFE extract, the encapsulated product and the non-encapsulated fraction from *D. salina*. Values in brackets show the encapsulation efficiency

| Peak ID | Rt (min) | Identification | Selected ion (*m/z*) | Main fragments (*m/z*) | Starting UHP-SFE extract ($\times 10^6$) | Non-encapsulated fraction ($\times 10^6$) | Encapsulated product ($\times 10^6$) (Encapsulation efficiency) | Sum of the non-encapsulated and encapsulated fractions |
|---|---|---|---|---|---|---|---|---|
| **Monoterpenes** | | | | | | | | |
| 2 | 11.03 ± 0.01 | *3,3-Dimethyl-2,7-octanedione* | 198 | 142, 99, 71, 43 | 4.96 ± 0.24 | 1.44 ± 0.08 | 0.69 ± 0.02 (14%) | 2.13 ± 0.10 |
| 3 | 13.86 ± 0.01 | *β-ionone* | 192 | 177, 149, 135, 93, 91, 43 | 2.06 ± 0.05 | 0.44 ± 0.04 | n.i. (0%) | 0.44 ± 0.04 |
| 5 | 15.99 ± 0.01 | *3-oxo-β-ionone* | 206 | 162, 43 | 2.46 ± 0.03 | 1.02 ± 0.06 | n.i. (0%) | 1.02 ± 0.06 |
| | | | | $\Sigma_{\text{volatile fraction}}$ = | 9.48 ± 0.32 | 2.9 ± 0.18 | 0.69 ± 0.02 (7%) | 3.59 ± 0.20 |
| **Diterpenes** | | | | | | | | |
| 6 | 18.60 ± 0.01 | *Neophytadiene* | 278 | 95, 83, 81, 68, 57 | 37.73 ± 1.60 | 0.57 ± 0.01 | n.i. (0%) | 0.57 ± 0.01 |
| 10 | 25.75 ± 0.01 | *Phytol* | 296 | 137, 123, 71, 57 | 3.99 ± 0.41 | 1.95 ± 0.01 | 0.51 ± 0.01 (13%) | 2.69 ± 0.02 |
| | | | | $\Sigma_{\text{volatile fraction}}$ = | 41.72 ± 2.01 | 2.52 ± 0.02 | 0.51 ± 0.01 (1%) | 3.26 ± 0.03 |
| **Sesquiterpenes** | | | | | | | | |
| 7 | 18.68 ± 0.01 | *Nerolidol* | 222 | 189, 161, 107, 81, 67, 43 | 2.71 ± 0.21 | 1.32 ± 0.01 | n.i. (0%) | 1.32 ± 0.01 |
| 14 | 29.22 ± 0.01 | *α-Cedrol* | 222 | 151, 135, 97, 41 | 61.94 ± 1.70 | 1.51 ± 0.01 | 0.76 ± 0.01 (1%) | 2.27 ± 0.02 |
| | | | | $\Sigma_{\text{volatile fraction}}$ = | 64.65 ± 1.91 | 2.83 ± 0.02 | 0.76 ± 0.01 (1%) | 3.59 ± 0.03 |
| **Triterpenes** | | | | | | | | |
| 17 | 30.79 ± 0.01 | *α-tocopherol* | 430 | 205, 177, 165, 121, 95, 71, 43 | 48.71 ± 2.94 | 0.59 ± 0.01 | 0.24 ± 0.02 (< 1%) | 0.83 ± 0.03 |
| 18 | 30.87 ± 0.01 | *β-sitosterol* | 414 | 396, 329, 303, 255, 213, 173, 145, 119, 105, 81, 43 | 5.65 ± 0.38 | 0.53 ± 0.01 | 0.03 ± 0.01 (1%) | 0.56 ± 0.02 |
| 19 | 30.95 ± 0.01 | *7-ergostenol* | 400 | 367, 315, 289, 255, 231, 173, 145, 119, 95, 81, 43 | 9.91 ± 0.54 | 0.50 ± 0.01 | 0.21 ± 0.01 (2%) | 0.71 ± 0.02 |
| 20 | 31.03 ± 0.01 | *Stigmasterol* | 412 | 351, 300, 213, 173, 159, 133, 91, 83, 55 | 5.19 ± 0.53 | 1.71 ± 0.06 | 0.22 ± 0.02 (4%) | 1.93 ± 0.08 |
| 21 | 31.13 ± 0.01 | *Stigmasta-4, 7, 22-trien-3-α-ol* | 414 | 396, 303, 255, 229, 145, 133, 95, 81, 43 | 2.77 ± 0.19 | 1.25 ± 0.10 | 0.14 ± 0.01 (5%) | 1.39 ± 0.11 |
| 22 | 32.00 ± 0.01 | *Spathulenol* | 220 | 220, 205, 159, 145, 105, 91, 55, 43 | 6.04 ± 0.08 | 0.65 ± 0.01 | 0.05 ± 0.01 (1%) | 0.70 ± 0.02 |
| 23 | 32.74 ± 0.04 | *Clionasterol* | 413 | 213, 105, 91, 78, 55, 43 | 16.63 ± 2.05 | 0.16 ± 0.01 | 0.42 ± 0.01 (1%) | 0.70 ± 0.02 |

**Table 3** (continued)

| Peak ID | Rt (min) | Identification | Selected ion (*m/z*) | Main fragments (*m/z*) | Starting UHP-SFE extract ($\times 10^6$) | Non-encapsulated fraction ($\times 10^6$) | Encapsulated product ($\times 10^6$) (Encapsulation efficiency) | Sum of the non-encapsulated and encapsulated fractions |
|---|---|---|---|---|---|---|---|---|
| 24 | 32.83 ± 0.05 | *Fucosterol* | 412 | 314, 299, 229. 272, 105, 43 | 8.81 ± 0.18 | 0.25 ± 0.01 | 0.52 ± 0.02 (6%) | 0.77 ± 0.03 |
| 25 | 32.98 ± 0.10 | *δ-tocopherol* | 430 | 205, 177, 185, 136, 95, 69, 43 | 4.58 ± 0.47 | 0.32 ± 0.01 | 0.42 ± 0.05 (9%) | 0.74 ± 0.06 |
| | | | | $\Sigma_{\text{volatile fraction}}$ = | 108.29 ± 7.36 | 5.96 ± 0.32 | 2.25 ± 0.16 (2%) | 90.50 ± 0.39 |
| **Other compounds** | | | | | | | | |
| | 8.37 ± 0.17 | *Glycerol* | 92 | 74, 61, 43 | 7.84 ± 0.70 | 1.41 ± 0.04 | 0.15 ± 0.01 (2%) | 1.56 ± 0.05 |
| *4* | 14.55 ± 0.01 | *5,6,7,7a-tetrahydro-4,4,7a-trimethyl-2(4H)-benzofuranone* | 180 | 152, 137, 111, 67, 43 | 3.37 ± 0.37 | 1.00 ± 0.04 | n.i (0%) | 1.00 ± 0.04 |
| *8* | 19.00 ± 0.01 | *9-hexadecanoic ethyl ester* | 282 | 199, 157, 129, 97, 73, 43 | 38.13 ± 0.58 | 1.60 ± 0.03 | 0.33 ± 0.05 (< 1%) | 1.93 ± 0.08 |
| *9* | 24.17 ± 0.01 | *Hecadecanoic acid* | 256 | 239, 213, 171, 157, 129, 98, 73, 57, 43 | 7.34 ± 0.13 | 1.20 ± 0.01 | 0.34 ± 0.04 (5%) | 1.54 ± 0.05 |
| *11** | 28.38 ± 0.13 | *9,12,15-Octadecatrienoic acid (Z, Z, Z)* | 264 | 208, 149, 93, 79, 41 | 1.67 ± 0.03 | 1.03 ± 0.08 | 0.72 ± 0.05 (43%) | 1.75 ± 0.13 |
| *12* | 28.72 ± 0.01 | *Phthalic acid* | 362 | 279, 251, 149, 122, 104, 85, 43 | 8.17 ± 0.23 | 1.17 ± 0.04 | 0.09 ± 0.01 (1%) | 1.26 ± 0.05 |
| *13** | 28.93 ± 0.01 | *Dodecyl 2-ethylhexyl ester* | 292 | 264, 243, 235, 150, 93, 67, 55 | 2.41 ± 0.25 | 2.54 ± 0.11 | 0.18 ± 0.01 (7%) | 2.72 ± 0.22 |
| *15* | 30.27 ± 0.01 | *9,12,15-octadecatrienoic acid methyl ester* | 294 | 121, 93, 80, 41 | 3.30 ± 0.01 | 0.59 ± 0.03 | 0.32 ± 0.02 (10%) | 0.91 ± 0.05 |
| *16* | 30.70 ± 0.01 | *1H-indole derivative* | 247 | 248, 203, 130. 105, 73, 43 | 3.36 ± 0.18 | 0.46 ± 0.04 | 0.21 ± 0.01 (6%) | 0.67 ± 0.05 |
| | | | | $\Sigma_{\text{volatile fraction}}$ = | 75.59 ± 8.78 | 11.00 ± 0.42 | 2.34 ± 0.20 (3%) | 13.34 ± 0.62 |

identified compound are summarized in Table 4. As can be deduced from these results, each process step caused a significant reduction in the number of compounds present in the fraction. The fraction obtained after steps II–IV presented losses of around 20% in the total content of compounds compared to the starting extract. These compound losses would be due to the formation of the emulsion and the applied conditions in this step (60 °C, 2 h). However, more pronounced decreases were observed in step V where compound reductions reached 68% (in comparison to step IV). Thus, the main parameters that affected both the encapsulation efficiency and the stability of the volatile compounds along the encapsulation steps were temperature and time in the different steps; this is crucial information to consider for further development of encapsulation processes regarding volatile terpenoids.

**Table 4** GC–MS study of the UHP-SFE extract evolution during the microencapsulation process for volatile compounds

| Peak ID | Rt (min) | Identification | Peak area ($\times 10^6$) | | | |
|---|---|---|---|---|---|---|
| | | | Starting extract | Step II-IV | Step V | Step VI |
| ***1*** | 8.374 ± 0.17 | *Glycerol* | 7.84 ± 0.70 | 1.78 ± 0.04* | 1.63 ± 0.06* | 1.59 ± 0.01* |
| ***2*** | 11.03 ± 0.01 | *3,3-Dimethyl-2,7-octanedione* | 4.96 ± 0.24 | 4.17 ± 0.09* | 2.45 ± 0.04* | 1.93 ± 0.05* |
| ***3*** | 13.86 ± 0.01 | *β-ionone* | 2.06 ± 0.05 | 2.28 ± 0.18 | 1.96 ± 0.01* | 0.44 ± 0.04* |
| ***4*** | 14.55 ± 0.01 | *5,6,7,7a-tetrahydro-4,4,7a-trimethyl-2(4H)-benzofuranone* | 3.37 ± 0.37 | 2.87 ± 0.12* | 2.65 ± 0.03* | 1.00 ± 0.04* |
| ***5*** | 15.99 ± 0.01 | *3-oxo-β-ionone* | 2.46 ± 0.03 | 2.12 ± 0.22* | 1.05 ± 0.01* | 1.04 ± 0.06 |
| ***6*** | 18.60 ± 0.01 | *Neophytadiene* | 37.73 ± 1.60 | 12.83 ± 0.54* | 0.59 ± 0.01* | 0.55 ± 0.03 |
| ***7*** | 18.68 ± 0.01 | *Phytol* | 2.71 ± 0.21 | 2.78 ± 0.25 | 1.34 ± 0.03* | 1.37 ± 0.09 |
| ***8*** | 19.00 ± 0.01 | *9-hexadecanoic ethyl ester* | 38.13 ± 0.58 | 37.82 ± 1.34 | 10.45 ± 0.02* | 6.69 ± 0.03* |
| ***9*** | 24.17 ± 0.01 | *Hexadecanoic acid methyl ester* | 7.34 ± 0.13 | 1.98 ± 0.10* | 1.87 ± 0.01 | 1.90 ± 0.05 |
| ***10*** | 25.75 ± 0.01 | *9,12,15-octadecatrienoic acid methyl ester* | 3.99 ± 0.41 | 3.17 ± 0.15* | 3.07 ± 0.01 | 2.55 ± 0.10* |
| ***11*** | 28.38 ± 0.13 | *9,12,15-octadecatrienoic acid (Z, Z, Z)* | 1.67 ± 0.03 | 1.77 ± 0.12 | 1.62 ± 0.14 | 1.77 ± 0.04 |
| ***12*** | 28.72 ± 0.01 | *Retinol* | 8.17 ± 0.23 | 1.65 ± 0.01* | 1.22 ± 0.10* | 1.26 ± 0.07 |
| ***13*** | 28.93 ± 0.01 | *Terephthalic acid, dodecyl 2-ethylhexyl ester* | 2.41 ± 0.25 | 1.34 ± 0.01* | 0.60 ± 0.05* | 0.39 ± 0.05* |
| ***14*** | 29.22 ± 0.01 | *Hexadecanoic acid* | 61.94 ± 1.70 | 62.37 ± 1.75 | 11.61 ± 0.01* | 2.59 ± 0.27* |
| ***15*** | 30.27 ± 0.01 | *Nerolidol* | 3.30 ± 0.01 | 1.79 ± 0.27* | 0.57 ± 0.03* | 0.55 ± 0.05 |
| ***16*** | 30.70 ± 0.01 | *1H-indole derivative* | 3.36 ± 0.18 | 3.33 ± 0.06 | 1.13 ± 0.03* | 1.12 ± 0.02 |
| ***17*** | 30.79 ± 0.01 | *α-tocopherol* | 5.65 ± 0.38 | 2.82 ± 0.19* | 1.71 ± 0.02* | 1.71 ± 0.03 |
| ***18*** | 30.87 ± 0.01 | *Ergosterol* | 5.19 ± 0.53 | 4.53 ± 0.24* | 2.96 ± 0.05* | 2.01 ± 0.01* |
| ***19*** | 30.95 ± 0.01 | *7-ergostenol* | 48.71 ± 2.94 | 51.70 ± 3.81 | 2.11 ± 0.02* | 1.56 ± 0.05* |
| ***20*** | 31.03 ± 0.01 | *Stigmasterol* | 9.91 ± 0.54 | 4.49 ± 0.12* | 2.44 ± 0.03* | 1.44 ± 0.03* |
| ***21*** | 31.13 ± 0.01 | *Stigmasta-4,7,22-trien-3-α-ol* | 2.77 ± 0.19 | 2.09 ± 0.07* | 1.29 ± 0.10* | 1.31 ± 0.21 |
| ***22*** | 32.00 ± 0.01 | *Spathunelol* | 6.04 ± 0.08 | 1.78 ± 0.01* | 1.24 ± 0.05* | 0.71 ± 0.02* |
| ***23*** | 32.74 ± 0.04 | *Clionasterol* | 16.63 ± 2.05 | 13.58 ± 0.08* | 13.60 ± 0.83 | 0.32 ± 0.01* |
| ***24*** | 32.83 ± 0.05 | *Fucosterol* | 8.81 ± 0.18 | 8.84 ± 0.61 | 2.39 ± 0.04* | 0.77 ± 0.04* |
| ***25*** | 32.98 ± 0.10 | *δ-tocopherol* | 4.58 ± 0.47 | 4.52 ± 0.21 | 3.86 ± 0.05* | 1.39 ± 0.04* |

*means significant differences ($p$-value<0.05) compared with the previous step

### In Vitro Neuroprotective Assessment of the Encapsulated Product

Encapsulation processes are carried out mainly to increase the stability of the compounds as well as to serve as a protection mechanism to avoid their biological and physical–chemical degradation. However, as mentioned previously, liposomal encapsulation technology is a method that could add other advantages like the protection of a bioactive ingredient throughout the gastrointestinal digestion process as well as to increase its bioaccessibility and bioavailability (González Gómez et al., 2019). For this reason, the neuroprotective potential of the encapsulated product was evaluated in this work, to study the feasibility of the applied encapsulation process to produce a bioactive ingredient. To describe the overall neuroprotective potential of the encapsulated product, different in vitro assays were selected, according to various mechanisms of action implicated in neurodegenerative diseases, i.e., anticholinesterase activity, anti-inflammatory capacity, and antioxidant activity.

Anticholinergic activity has previously been related to the normal maintenance of acetylcholine levels in the brain, as it has been observed that levels of this metabolite in Alzheimer's patients, among other neurological disorders, are significantly reduced. In the present work, the potential acetylcholinesterase (AChE) and butyrylcholinesterase (BuChE) enzymes inhibition activities of the encapsulated product were studied. The results obtained are illustrated in Fig. 3C. As can be observed, the encapsulated product showed significantly lower AChE and BuChE activities than the starting UHP-SFE *D. salina* extract. Particularly, a reduction of the AChE inhibition from 52.06 ± 5.32 mg-eq galantamine $g^{-1}$ extract to 32.69 ± 3.37 mg-eq galantamine $g^{-1}$ extract was observed. A lower decrease was found for BuChE enzyme, from 28.20 ± 2.25 mg-eq galantamine $g^{-1}$ extract for the starting UHP-SFE extract to 24.42 ± 2.00 mg-eq galantamine $g^{-1}$ extract for the encapsulated product. Interestingly, the AChE inhibition values of the encapsulated product were around 63% of the activity of the starting extract. This value is very close to

the total carotenoid encapsulation efficiency obtained, indicating that most of AChE inhibitory action would correspond to the carotenoids present in the extracts. On the other hand, considering the reduction of 13% observed for BuChE inhibition activity, other components also present in the extract could have a direct influence on the activity of this enzyme.

The anti-inflammatory capacity of both, the starting UHP-SFE extract and the encapsulated product, is shown in Fig. 3D. Comparing both results, the encapsulated extract suffered a loss of 22% bioactivity compared to the original extract ($4.89 \pm 0.37$ and $6.31 \pm 0.53$ mg-eq quercetin $g^{-1}$ extract).

Finally, the antioxidant activity of the different extracts was studied following four different methods. Regarding ROS inhibition (Fig. 3E), the encapsulated extract showed a decrease in its activity of almost 60% of the original UHP-SFE extract. This decrease could be related to the high correlation between ROS inhibition and carotenoids presented in this extract (Amador-Luna et al., 2024). This, in addition, could explain the lower general activity of *D. salina* extracts against these reactive species, due to the scarce presence of short-chain terpene compounds. This was particularly observed in the encapsulated product, where no monoterpene compounds were found. Regarding RNS scavenging (Fig. 3E), the encapsulation process produced a loss of 40%, with a value of $1.50 \pm 0.20$ mg-eq ascorbic acid $g^{-1}$ extract. This value presented a similar trend to the percentage of encapsulation of total terpenes, which may confirm that, in the case of the RNS scavenging, terpenes were one of the main components that influenced this bioactivity.

Focusing on the antioxidant capacity of the free radicals (Fig. 3F), it was possible to appreciate that the bioactivity related to the ABTS radical of the encapsulated product suffered a loss of 40% ($168 \pm 10$ µmol-eq Trolox $g^{-1}$ extract vs. $280 \pm 2$ µmol-eq Trolox $g^{-1}$ extract); that result showed a response similar to the RNS inhibition, which could be due to the encapsulation efficiency of total terpenes which are the most important bioactive compounds presented in UHP-SFE extracts (Amador-Luna et al., 2024). Finally, in the case of the DPPH radical, the encapsulated product presented an activity of $132 \pm 7$ µmol-eq Trolox $g^{-1}$ extract, a value 46% lower than the original extract. These results are in agreement with the encapsulation efficiency results, considering that the main scavenging activity has been related to β-carotene isomers that presented an encapsulation efficiency of around 51% (Müller et al., 2002).

The obtained results indicated that the encapsulation process produced a notable loss of activity in comparison to the starting extract; however, despite this loss of bioactivity, the obtained results of the final encapsulated product presented a great neuroprotective capacity. In fact, the results observed for the anticholinergic, anti-inflammatory and antioxidant activity of the encapsulated product, were higher than those observed in previous works for free *D. salina* extracts obtained under conventional pressure SFE (Amador-Luna et al., 2024; Bueno et al., 2020).

### Stability Study

The stability of the starting *D. salina* UHP-SFE extract and the encapsulated product was studied over time using controlled atmospheric conditions. Moreover, the encapsulation product was submitted to accelerated conditions (45 °C) as well. Results obtained from this study are presented in Fig. 4. The stability of both extracts was estimated in terms of TCC, as well as in terms of AChE inhibitory activity. As can be seen in Fig. 4A, a rapid degradation of the carotenoids present in the starting extract as well as a significant decrease in its AChE inhibition activity were observed at room conditions; in this sense, TCC was reduced by 59% in just 7 days, and a complete degradation was observed after 21 days. The same trend was followed by the AChE inhibition activity, showing once more the high correlation between carotenoids present in the extract and this activity. On the other hand, TCC and activity of the encapsulated product remained constant in all the tests carried out at room conditions, without showing significant differences in any of the measurements compared to the initial point measurement (0 days).

In the case of the evaluation of the accelerated conditions on the stability of the encapsulated process (Fig. 4B), a slight decrease in the concentration of carotenoids and bioactivity was observed over time, corresponding to a loss of 20% of carotenoids and a 21% reduction of the initial bioactivity throughout the entire period (3 months). These results are in agreement with other stability studies of liposomal microencapsulates, in which the presence of the components of interest was maintained without significant differences until the first month (Katragadda et al., 1999). In general, the results obtained in this work show that the developed encapsulation process is a useful means to maintain the stability, chemical composition and bioactivity of natural carotenoid-rich extracts over time.

## Conclusions

The present study demonstrates the suitability of a liposome-based microencapsulation process to efficiently protect the bioactive carotenoid-rich natural extract obtained from *D. salina* using UHP-SFE. A six-step process based on the use of phosphatidylcholine as encapsulating agent allowed the encapsulation of the most bioactive extract components. The encapsulated extract presented an encapsulation efficiency of 63%, which coincided with the observed percentage of the overall neuroprotective activity of the encapsulated product. The evaluation of the effect of each step allowed determining that the main affected compounds were the volatile terpenes probably due to the temperatures used in the process, especially a

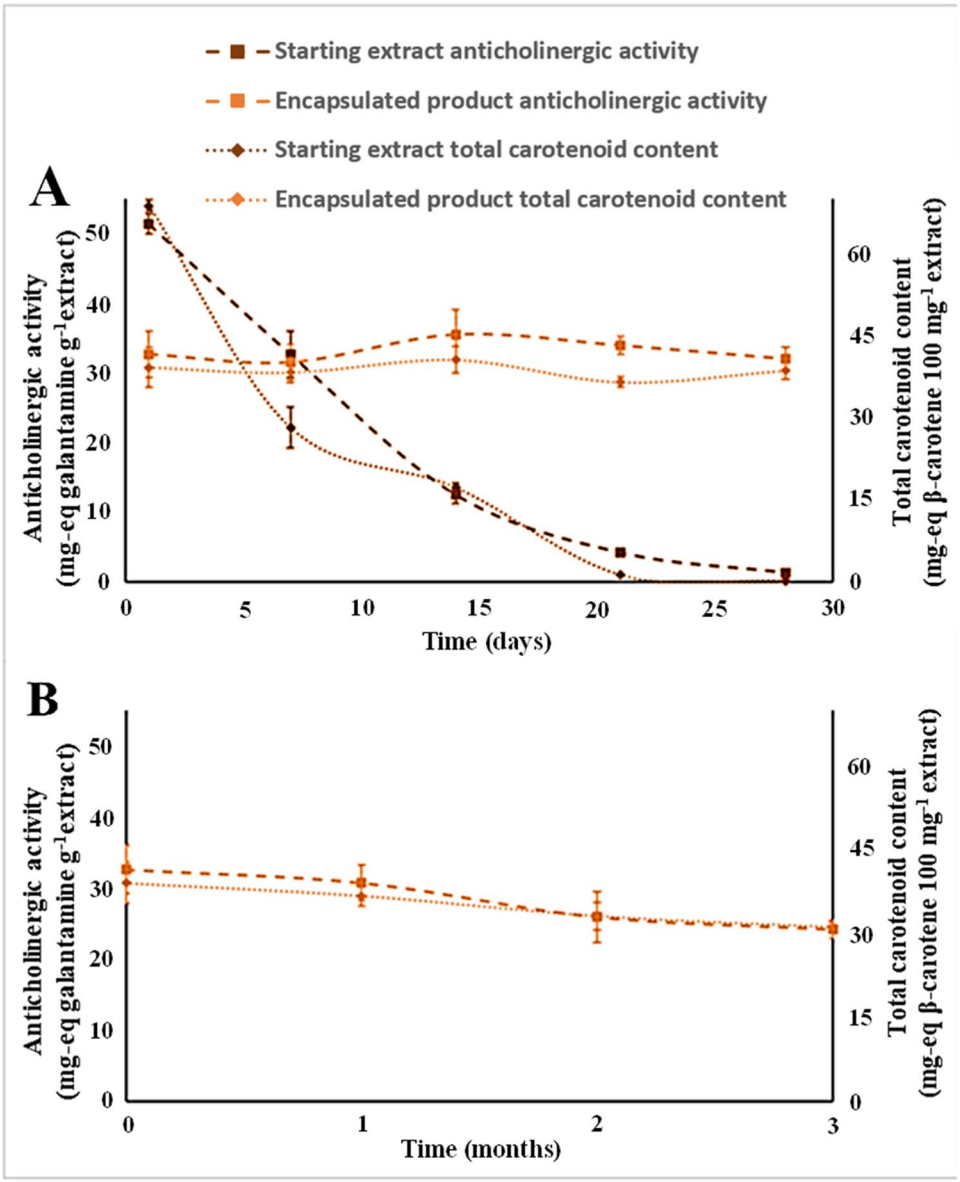


**Fig. 4** Stability of the in vitro neuroprotection (AChE inhibition) and TCC for the starting UHP-SFE non-encapsulated extract (brown) and the UHP-SFE encapsulated product (orange) along the time in **A** simple (21 °C, 0.1 MPa and 50% relative humidity) and **B** accelerated conditions (45 °C, 0.1 MPa, and 75% relative humidity)

significant reduction of these compounds was observed during the purification step. On the other hand, carotenoids showed an encapsulation efficiency of 56%, but they did not suffer degradation during the encapsulation process (showing the remaining carotenoid content intact and present in the non-encapsulated fraction). Considering the 63% efficiency, the encapsulation method was demonstrated to be effective in preserving the extract composition and bioactivity values over long periods.

Although the process is suitable for producing bioactive ingredients with proper stability over time, further research efforts should be focused on an optimization of the whole encapsulation process, and even more in the emulsion formation process, to improve the liposomal encapsulation to reduce the terpene degradation and to increase the carotenoid encapsulation efficiency.

**Supplementary Information** The online version contains supplementary material available at https://doi.org/10.1007/s11947-025-03820-x.

**Author Contribution** V.M.A-L: conceptualization, methodology, validation, formal analysis, investigation, writing – original draft, visualization. M.H.: conceptualization, resources, writing – review & editing, supervision, project administration, funding acquisition. P.M.-O: validation, investigation. E.I.: resources, writing – review & editing, project administration. L.M.: conceptualization, validation, investigation, resources, writing – review & editing, visualization, supervision, project administration.

**Funding** Open Access funding provided thanks to the CRUE-CSIC agreement with Springer Nature. V.M.A-L. acknowledges the "Formación del Profesorado Universitario" grant (FPU21/00054) funded by the Spanish Ministry of Universities. L.M. acknowledges the "Ramon y Cajal" grant (RYC2021-033148-I) funded by MCIN/AEI/https://doi.org/10.13039/501100011033 and by "European Union NextGenerationEU/PRTR." This work was supported by grants

PID2020-113050RB-I00 and PDC2021-120814-I00 funded by MCIN/AEI/https://doi.org/10.13039/501100011033 (Spain) and European Union "NextGenerationEU"/PRTR."

**Data Availability** The authors declare that the data supporting the findings of this study are available within the paper and its Supplementary Information files. Should any raw data files be needed in another format, they are available from the corresponding author upon reasonable request.No datasets were generated or analysed during the current study.

## Declarations

**Ethical Approval** The study involved no experimentation with human subjects.

**Consent to Participate** The authors declare their consent to participate in this article.

**Consent for Publication** The authors declare their consent to publish in this article.

**Conflict of Interest** The authors declare no conflict of interest.

**Open Access** This article is licensed under a Creative Commons Attribution 4.0 International License, which permits use, sharing, adaptation, distribution and reproduction in any medium or format, as long as you give appropriate credit to the original author(s) and the source, provide a link to the Creative Commons licence, and indicate if changes were made. The images or other third party material in this article are included in the article's Creative Commons licence, unless indicated otherwise in a credit line to the material. If material is not included in the article's Creative Commons licence and your intended use is not permitted by statutory regulation or exceeds the permitted use, you will need to obtain permission directly from the copyright holder. To view a copy of this licence, visit http://creativecommons.org/licenses/by/4.0/.

## References

Akanda, M., Mithu, S. H., & M. D., Douroumis, D. (2023). Solid Lipid nanoparticels: An effective lipid-based technology for cancer treatment. *Journal of Drug Delivery Science and Technology., 86*,. https://doi.org/10.1016/j.jddst.2023.104709

Akram, N., Afzaal, M., Saeed, F., Shah, Y. A., Faisal, Z., Asghar, A., Ateeq, H., Nayik, G. A., Wani, S. H., Hussain, M., Shah, M. A., & Khaneghah, A. M. (2023). Liposomes: A promising delivery systema for active ingredients in food and nutrition. *International Journal of Food Properties., 26*(1), 2476–2492. https://doi.org/10.1080/10942912.2023.2247578

Alharbi, W. S., Almughem, F. A., Almehmady, A. M., Jarallah, S. J., Alsharif, W. K., Alzahrani, N. M., & Alshehri, A. A. (2021). Phytoshomes as an emerging nanotechnology platform for the tropical delivery of bioactive phytochemicals. *Pharmaceutics., 13*(9), 1475. https://doi.org/10.3390/pharmaceutics13091475

Amador-Luna, V. M., Herrero, M., Domínguez-Rodríguez, G., Ibáñez, E., & Montero, L. (2024). Enhancing the bioactivity of *Dunaliella salina* extracts through ultra-high pressure supercritical fluid extraction (UHP-SFE). *Innovative Food Science and Emerging Technologies., 95*,103697 https://doi.org/10.1016/j.ifset.2024.103697

Andleeb, M., Shoaib Khan, H. M., Daniyal, M. (2021). Development, characterization and stability evaluation of topical gel loaded with ethosomes containing *Achillea millefolium* L. extract. *Frontiers in Pharmacology. 12,* 603227. https://doi.org/10.3389/fphar.2021.603227.

Beyrami, M., Karimi, E., & Oskoueian, E. (2020). Synthesized chrysin-loaded nanoliposomes improves cadmium-induced toxicity in mice. *Environmental Science and Pollution Research., 27*, 40643–40651. https://doi.org/10.1007/s11356-020-10113-7

Bueno, M., Vitali, C., Sánchez-Martínez, J. D., Mendiola, J. A., Cifuentes, A., Ibáñez, E., & Herrero, M. (2020). Compressed $CO_2$ technologies for the recovery of carotenoid-enriched extracts from *Dunaliella salina* with potential neuroprotective activity. *ACS Sustainable Chemical Engineering, 8*(30), 11413–11423. https://doi.org/10.1021/acssuschemeng.0c03991

Cheng, X., Yan, H., Pang, S., Ya, M., Qiu, F., Qin, P., Zeng, C., & Lu, Y. (2022). Liposomes as multifunctional nano-carriers for medicinal natural products. *Frontiers in Chemistry., 10*,. https://doi.org/10.3389/fchem.2022.963004

Davidov-Pardo, G., Joye, I., & McClements, D. (2015). Encapsulation of resveratrol in biopolymer particles produced using liquid antisolvent precipitation. Part 1: Preparation and characterization. *Food Hydrocolloids, 45*, 309–316. https://doi.org/10.1016/j.foodhyd.2014.11.023

Déclaire Mabou, F., & Nzeuwa Yossa, I. B. (2021). Terpenes: Structural classification and biological activities. *IOSR Journal of Pharmacy and Biological Sciences., 16*(3), 25–40. https://doi.org/10.9790/3008-1603012540

Desai, M. P., Labhasetwar, V., Amidon, G. L., & Lavy, R. J. (1996). Gastrointestinal uptake of biodegradable microparticles: Effect of particle size. *Pharmaceutical Research., 13*, 1838–1845. https://doi.org/10.1023/A:1016085108889

Fang, Z., & Bhandari, B. (2010). Encapsulation of polyphenols. *Trends in Food Science & Technology., 21*(10), 510–523. https://doi.org/10.1016/j.tifs.2010.08.003

FDA (2018). Liposome drug products chemistry, manufacturing, and controls; human pharmacokinetics and bioavailability; and labeling documentation. Center for Drug Evaluation and Research. U.S. Department of Health and Human Services.

Fei, T., Gwinn, K., Leyva-Gutierrez, F. M. A., & Wang, T. (2023). Nanoemulsions of terpene by-products from cannbidiol production have promising insecticidal effect on *Callosobruchus maculatus*. *Cell Press., 9*(4). https://doi.org/10.1016/j.heliyon.2023.e15101

Gallego, R., Valdés, A., Sánchez-Martínez, J. D., Suárez Montenegro, Z. J., Ibáñez, E., Cifuentes, A., & Herrero, M. (2022). Study of the potential neuroprotetive effect of *Dunaliella salina* extract in SH-SY5Y cell model. *Analytical and Bioanalytical Chemistry, 414*, 5357–5371. https://doi.org/10.1007/s00216-021-03819-1

Ge, X., Wei, M., He, S., & Yuan, W.-E. (2019). Advances of non-ionic surfactant vesicles (niosomes) and their application in drug delivery. *Pharmaceutics., 11*(2), 55. https://doi.org/10.3390/pharmaceutics11020055

Gonzalez Gomez, A., Syed, S., Marshall, K., & Hosseinidoust, Z. (2019). Liposomal nanovesicles for efficient encapsulation of Staphylococcal antibiotics. *ACS Omega, 4*(6), 10866–10876. https://doi.org/10.1021/acsomega.9b00825

Harnkarnsujarit, N., Charoenrein, S., & Roos, Y. H. (2012). Microstructure formation of maltodextrin and sugar matrices in freeze-dried systems. *Carbohydrate Polymers., 88*(2), 734–742. https://doi.org/10.1016/j.carbpol.2012.01.028

Kaltschmidt, B. P., Ennen, I., Greiner, J. F. W., Dietsch, R., Patel, A., Kaltschmidt, B., Kaltschmidt, C., Hütten, A. (2020). Preparation of terpenoid-invasomes with selective activity against *S. aureus* and characterization by cryo transmission electron microscopy. *Biomedicines. 8* (5), 105. https://doi.org/10.3390/biomedicines8050105.

Katragadda, A. K., Singh, M., & Betageri, G. V. (1999). Encapsulation, stability and in vitro release characteristics of liposomal formulations of stavudine (D4T). *Drug Delivery, 6*(1), 31–37. https://doi.org/10.1080/107175499267138

Kosaraju, S. L., Tran, C., & Lawrence, A. (2008). Liposomal delivery systems for encapsulation of ferrous sulfate: Preparation and characterization. *Journal of Liposome Research, 16*(4), 347–358. https://doi.org/10.1080/08982100600992351

Lason, E. (2020). Topical administration of terpenes encapsulated in nanostructured lipid-based systems. *Molecules, 25*(23), 5758. https://doi.org/10.3390/molecules2523575

Lavelli, V., & Sereikaitè, J. (2022). Kinetic study of encapsulation β-carotene in dried systems: A review. *Foods, 11*(3), 437. https://doi.org/10.3390/foods11030437

Magakian, D., Ocaña, S. D., Perez, C., & Banchio, C. (2021). Phosphatidylcholine restores neuronal plasticity of neural stem cells under inflammatory stress. *Scientific Reports., 11*, 22891. https://doi.org/10.1038/s41598-021-02361-5

Maoka, T. (2020). Carotenoids as natural functional pigments. *Journal of Natural Medecines, 74*, 1–16. https://doi.org/10.1007/s11418-019-01364-x

Mordi, R. C., Ademosun, O. T., Ajanaku, C. O., Afedolapo, O. O., & Walton, J. C. (2020). Free radical mediated degradation of carotenes and xantophylls. *Molecules, 25*(5), 1038. https://doi.org/10.3390/molecules25051038

Morris, V. J. (2014). Food technologies: Nanotechnology and food safety. *Encyclopedia of Food Safety., 3*, 208–210. https://doi.org/10.1016/B978-0-12-378612-8.00277-8

Müller, P., Li, X. P., & Niyogi, K. K. (2002). Non-photochemical quenching. A response to excess light energy. *Plant Physiology, 125*, 1558–1566. https://doi.org/10.1104/pp.125.4.1558

Olatunde, A., Tijjani, H., Ishola, A. A., Egbuna, C., Hassan, S., Akram, M. (2020). Carotenoids as functional bioactive compound. In: Dable Tupas G (ed) Egbuna C. *Functional Foods and Nutraceuticals Springer*, Cham. pp 415–444. https://doi.org/10.1007/978-3-030-42319-3_20.

Oskoueian, E., Karimi, E., Noura, R., Ebrahimi, M., Shafaei, N., & Karimi, E. (2020). Nanoliposomes encapsulation of enriched phenolic fraction from pistachio hulls and its antioxidant, anti-inflammatory and anti-melanogenic activities. *Journal of Microencapsulation, 37*(1), 1–13. https://doi.org/10.1080/02652048.2019.1692941

Ozkan, G., Franco, P., de Marco, I., Xiao, J., & Capanoglu, E. (2019). A review of microencapsulation methods for food antioxidants: Principles, advantages, drawbacks and applications. *Food Chemistry., 272*, 494–506. https://doi.org/10.1016/j.foodchem.2018.07.205

Rostamabadi, H., Falsafi, S. R., & Jarafi, S. M. (2019). Nanoencapsulation of carotenoids within lipid-based nanocarriers. *Journal of Controlled Release., 298*, 38–67. https://doi.org/10.1016/j.jconrel.2019.02.005

Sánchez-Martínez, J. D., Álvarez-Rivera, G., Gallego, R., Fagundes, M. B., Valdés, A., Mendiola, J. A., Ibañez, E., & Cifuentes, A. (2022). Neuroprotective potential of terpenoid-rich extracts from orange juice by-products obtained by pressurized liquid extraction. *Food Chemistry: X., 13*,. https://doi.org/10.1016/j.fochx.2022.100242

Sobel, R., Versic, R., Gaonkar, A. G. (2023) Chapter 1 – Introduction to microencpsulation and controlled delivery in foods. In: Sobel, R. (Ed.) Microencapsulation in the Food Industry (Second Edition). A Practical Implementation Guide. *Academic Press*. 1–9. https://doi.org/10.1016/B978-0-12-821683-5.00019-4.

Thies, C. (2012). Microencapsulation methods based on biopolymer phase separation and gelation phenomena in aqueous media. In: Garti, N., spsampsps McClements, D. J. (Eds.). (2012). Encapsulation technologies and delivery systems for food ingredients and nutraceuticals. *Woodhead Publishing Series in Food Science, Technology and Nutrition*. 177–207. https://doi.org/10.1533/9780857095909.2.177.

Valdés, A., Sánchez-Martínez, J. D., Gallego, R., Ibáñez, E., Herrero, M., & Cifuentes, A. (2024). In vivo neuroprotective capacity of a *Dunaliella salina* extract—Comprehensive transcriptomics and metabolomics study. *Npj Science of Food, 8*(4), 1–15. https://doi.org/10.1038/s41538-023-00246-7

Zhang, K., Zhang, Y., Li, Z., Li, N., & Feng, N. (2017). Essential oil-mediated glycerosomes increase transdermal paeoniflorin delivery: Optimization, characterization, an evaluation in vitro and in vivo. *International Journal of Nanomedecine, 5*(12), 3521–3532.

**Publisher's Note** Springer Nature remains neutral with regard to jurisdictional claims in published maps and institutional affiliations.